Christoph Prause, BSc

Mild Decarboxylation of Acrylic Acid Derivatives utilizing Ferulic Acid Decarboxylase from *Saccharomyces cerevisiae*: Substrate Scope and Enzyme Characterization in Regard to Synthetic Applications

MASTER'S THESIS

to achieve the university degree of

Master of Science

Master's degree programme: Chemistry

submitted to

Graz University of Technology

Supervisor

O.Univ.-Prof.i.R. Dr.phil. Kurt Faber

Department of Chemistry, University of Graz

Graz, February 2018

AFFIDAVIT

I declare that I have authored this thesis independently, that I have not used other than the declared sources/resources, and that I have explicitly indicated all material which has been quoted either literally or by content from the sources used. The text document uploaded to TUGRAZonline is identical to the present master‘s thesis.

Date

Signature

Danksagung

Meine innigste Dankbarkeit gilt

meinen Eltern, die auf jedem Schritt meines Weges für mich da waren,
meinem Großvater Hans, für seine Weisheit und rastlose Unterstützung,
meinen Freunden, die mir immer wieder neue Horizonte eröffnen,
meinen Betreuern Kathi und Kurt, für ihre Geduld und Hilfsbereitschaft,
sowie allen weiteren Mitgliedern der Elk-Crew, die mich als einen der ihren am Institut aufgenommen haben.

Ohne euch wäre ich niemals so weit gekommen. Bleibt wie ihr seid, denn ihr seid großartig.

Euer Christoph

Abstract

Ferulic acid decarboxylase (Fdc1) from the budding yeast *Saccharomyces cerevisiae* is well known to catalyze the redox-neutral decarboxylation of acrylic acid derivatives such as cinnamic acid, ferulic acid and sorbic acid, yielding the corresponding terminal alkenes styrene, 4-vinylguaiacol and 1,3-pentadiene.[1]

Terminal alkenes are highly relevant base chemicals that are consumed on a large scale in the industrial production of polymers and fine chemicals, while the bulk of their supply is derived from energy-intensive, non-renewable petrochemical processes.[2]

The goal of this thesis was to elucidate the range of application of Fdc1 in regard to substrate scope, reaction time, temperature stability, pH optimum and compatibility with organic solvents to examine the possibility for future implementations of this enzyme in preparative and industrial chemistry.

Zusammenfassung

Ferulasäure-Decarboxylase (Fdc1) der Sprosshefe *Saccharomyces cerevisiae* katalysiert die redox-neutrale Decarboxylierung von Acrylsäure-Derivaten wie Zimtsäure, Ferulasäure sowie Sorbinsäure und produziert somit die entsprechenden terminalen Alkene Styrol, 4-Vinylguajacol und 1,3-Pentadien.[1]

Terminale Alkene sind hochrelevante Basischemikalien welche in großem Maßstab in der industriellen Fertigung von Polymeren und Feinchemikalien verarbeitet werden, deren Herstellung allerdings nahezu ausschließlich auf energieintensiven, nicht erneuerbaren petrochemischen Prozessen beruht.[2]

Das Ziel dieser Arbeit bestand darin, den Anwendungsbereich von Fdc1 im Hinblick auf Substrat-Spektrum, Reaktionszeit, Temperaturstabilität, pH-Optimum sowie Kompatibilität mit organischen Lösungsmitteln zu erarbeiten, um die Möglichkeiten einer zukünftigen Anwendung dieses Enzyms in der präparativen und industriellen Chemie zu beleuchten.

Contents

1. Introduction

Shrinking fossil fuel reserves and increasing concerns about the release of harmful waste products into the environment have sparked interest in the development of more sustainable processes for the production of organic building blocks.[3] Biocatalytic approaches to this challenge are gaining more and more traction as enzymes and microorganisms can perform a wide variety of synthetically useful transformations and usually operate under mild reaction conditions with excellent control of chemo-, stereo- and regioselectivity, while unproductive protection and deprotection steps can often be circumvented.[4] Ferulic acid decarboxylase (Fdc1) from *S. cerevisiae* seems to be a promising candidate for this application since it catalyzes the redox-neutral decarboxylation of acrylic acid derivatives under ambient conditions, yielding terminal alkenes of potential industrial relevance. Recently published investigations by Payne *et al.* indicate that the enzymatic reaction mechanism involves a transient cycloadduct between one molecule of α,β-unsaturated substrate and the enzyme's cofactor, a newly discovered prenylated derivative of flavin mononucleotide (prFMN) with properties comparable to azomethine ylides, therefore characterizing the reaction as a 1,3-dipolar cycloaddition.[5] This type of transformation is commonly utilized in the laboratory synthesis of organic heterocycles, however enzymatic equivalents to it were previously unknown, making these findings a further expansion of the already rich biochemical knowledge about flavoproteins.[6] Herein, the windows of application for Fdc1 in regard to crucial parameters such as reaction time, temperature, pH and compatibility with organic co-solvents are reported. The enzyme's substrate scope in the decarboxylation direction was examined with 37 structurally diverse compounds, including acrylic acids substituted with aromatic heterocycles. From the obtained results and mechanistic considerations, minimal substrate requirements were delineated. Furthermore, the feasibility to use this enzyme in the carboxylation of terminal alkenes was tested with 4-vinylguaiacol, 1,3-pentadiene, isoprene and myrcene, utilizing $KHCO_3$ or pressurized CO_2 as potential C_1 donors. Conclusively, a preparative-scale biotransformation of ferulic acid to 4-vinylguaiacol was performed.

2. Theoretical Background

2.1. Significance of (de)carboxylation in natural systems

The release as well as the fixation of carbon dioxide constitute two of the most fundamental reaction types in biochemistry (Scheme 2.1). Decarboxylation of organic acids is involved in a plethora of biotransformations and essential metabolic pathways, including the generation of acetyl-CoA from pyruvate, its further breakdown in the tricarboxylic acid cycle and the generation of amine neurotransmitters from amino acids.[7] The thermodynamically favored release of CO_2 is often utilized as a driving force for endergonic bioreactions and can also be coupled to electron transfer. The reverse carboxylation reaction is of substantial importance as well, since the incorporation of CO_2 is often a crucial step to confer functionalization to a molecule, for example in the assimilation of unreactive substrates or *de novo* biosynthesis of fatty acids.[8] Most importantly, the photosynthetic fixation of CO_2 by autotrophic organisms through the Calvin cycle is the biosphere's paramount strategy to acquire inorganic carbon from the environment. The ubiquitous enzyme ribulose 1,5-bisphosphate carboxylase/oxygenase (RuBisCO) catalyzes the quintessential first step of the cycle and has been estimated to be the most abundant protein on planet earth.[9]

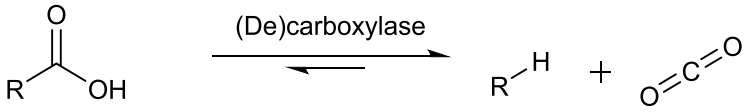

Scheme 2.1. General reaction scheme for enzymatic (de)carboxylation.

However, since C-C or C-H bond heterolysis is a necessary first step for the reaction to proceed in either direction, the transition state involves the highly disfavored buildup of negative charge at the α-carbon, which constitutes a significant kinetic barrier. Thus, most organic acids are stable molecules at physiological conditions and spontaneous decarboxylation is observed rather rarely. Nature has evolved a variety of different biocatalytic systems to overcome this obstacle by stabilization or circumvention of the high-energy carbanion state. (De)carboxylases have been discovered to utilize a large variety of organic prosthetic groups such as biotin, flavin, pyruvoyl groups, pyridoxal phosphate, thiamine pyrophosphate as well as divalent metal ions like Zn^{2+}, Mg^{2+}, Mn^{2+}, Fe^{2+} and Co^{2+}, but also redox-active nicotinamides when (de)carboxylation is coupled

to electron transfer.[1a, b] Cofactor-independent examples are known, but may depend on the presence of activating/stabilizing groups within the substrate molecule.

2.2. Applications of (de)carboxylases

The environmentally sustainable production of useful chemicals from natural materials has garnered much interest in recent years. The implementation of biocatalytic systems into industrial production routines is an ongoing trend, aiming at process optimization, reduction of cost and the prevention of harmful byproducts.[10] Within this discipline, the utilization of decarboxylases is a field of growing interest since these enzymes usually display excellent selectivity and operate under mild reaction conditions.[11]

In traditional chemical methodology, decarboxylation is viewed as an irreversible process because the liberated carboxylate group escapes the reaction mixture as gaseous CO_2, pushing the equilibrium towards the decarboxylated products. Nonetheless, the reverse carboxylation direction is feasible, with one of the most prominent examples being the Kolbe-Schmitt reaction applied in the industrial production of salicylic acid from alkali phenoxides.[12] Due to unfavorable reaction thermodynamics, the process requires harsh temperature and pressure to ensure acceptable product yields, resulting in high cost and energy demand. The application of enzymes as selective catalysts may offer an alternative approach to this synthetic challenge.[13]

When providing a large excess of CO_2 or an analog thereof such as bicarbonate, the reaction equilibrium is shifted by Le Chatelier effects towards the incorporation of CO_2 into the substrate molecule, enabling some decarboxylases to efficiently catalyze carboxylation under ambient conditions.[14] This approach provides a useful tool for selective substrate functionalization and may even open up synthetic strategies that are not feasible with traditional methods of organic chemistry, for example the regioselective β-carboxylation of styrene derivatives.[14c-e]

2.3. Overview of fungal Fdc1 and bacterial UbiD

Fdc1 is a three-domain, 56 kDa protein native to the yeast *S. cerevisiae*.[15] The enzyme catalyzes the redox-neutral decarboxylation of acrylic acid derivatives such as sorbic acid and ferulic acid, producing the corresponding terminal alkenes (Scheme 2.2). Due to their volatility and limited solubility in aqueous media, the decarboxylation products leave the cytosol by diffusion, suggesting the enzyme serves a function in cellular detoxification processes.[16]

Fdc1 is a member of the UbiD enzyme family, a set of related decarboxylases occurring in bacteria, fungi and archaea.[17] The canonical *E. coli* UbiD is involved in bacterial ubiquinone biosynthesis, catalyzing the decarboxylation of 3-octaprenyl-4-hydroxybenzoic acid to 2-octaprenylphenol (Scheme 2.2).[18]

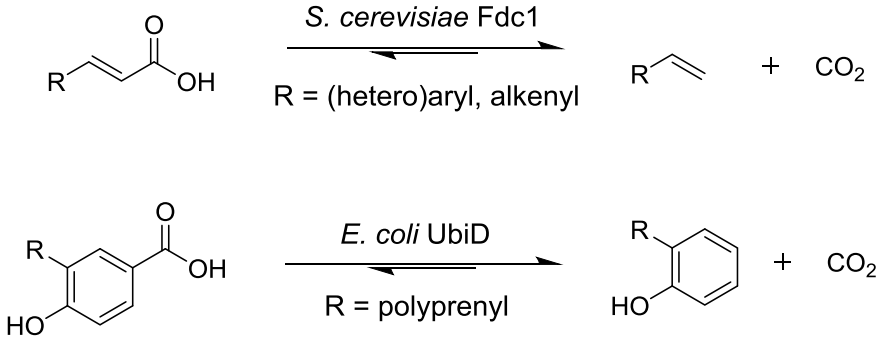

Scheme 2.2. Decarboxylation reactions catalyzed by *S. cerevisiae* Fdc1 and *E. coli* UbiD.

Recently, detailed investigations have established that members of the UbiD family require a newly discovered cofactor for activity, a prenylated derivative of flavin mononucleotide (prFMN).[5, 17] This compound displays unusual electronic properties comparable to 1,3-dipolar azomethine ylides and is biosynthesized by covalent modification of $FMNH_2$ catalyzed by prenyltransferase UbiX (*E. coli*) or the homologous Pad1 (*S. cerevisiae*), followed by oxidative maturation (Scheme 2.3).[19] The transformation initially links a prenyl C_5 unit to N5 and C6 on the flavin skeleton, forming a fourth, non-aromatic ring. Interestingly, UbiX does not utilize the common terpene donors dimethylallyl pyrophosphate (DMAPP) or isopentenyl pyrophosphate, but rather non-canonical dimethylallyl monophosphate. Pad1, on the other hand, preferentially binds the more common DMAPP as its co-substrate.[20] The resulting intermediate $prFMNH_2$ is oxidized by molecular oxygen within *holo*-Fdc1 to the catalytically active prFMN, which is a resonance-stabilized, nitrogen-centered 1,3-dipole. The generation of the catalytically competent species within the active site of Fdc1 is a reasonable proposition since dipolar prFMN is expected to be rather unstable under ambient conditions. This also suggests that the Fdc1 active site has to be kept free from external water to ensure the cofactor's structural integrity.

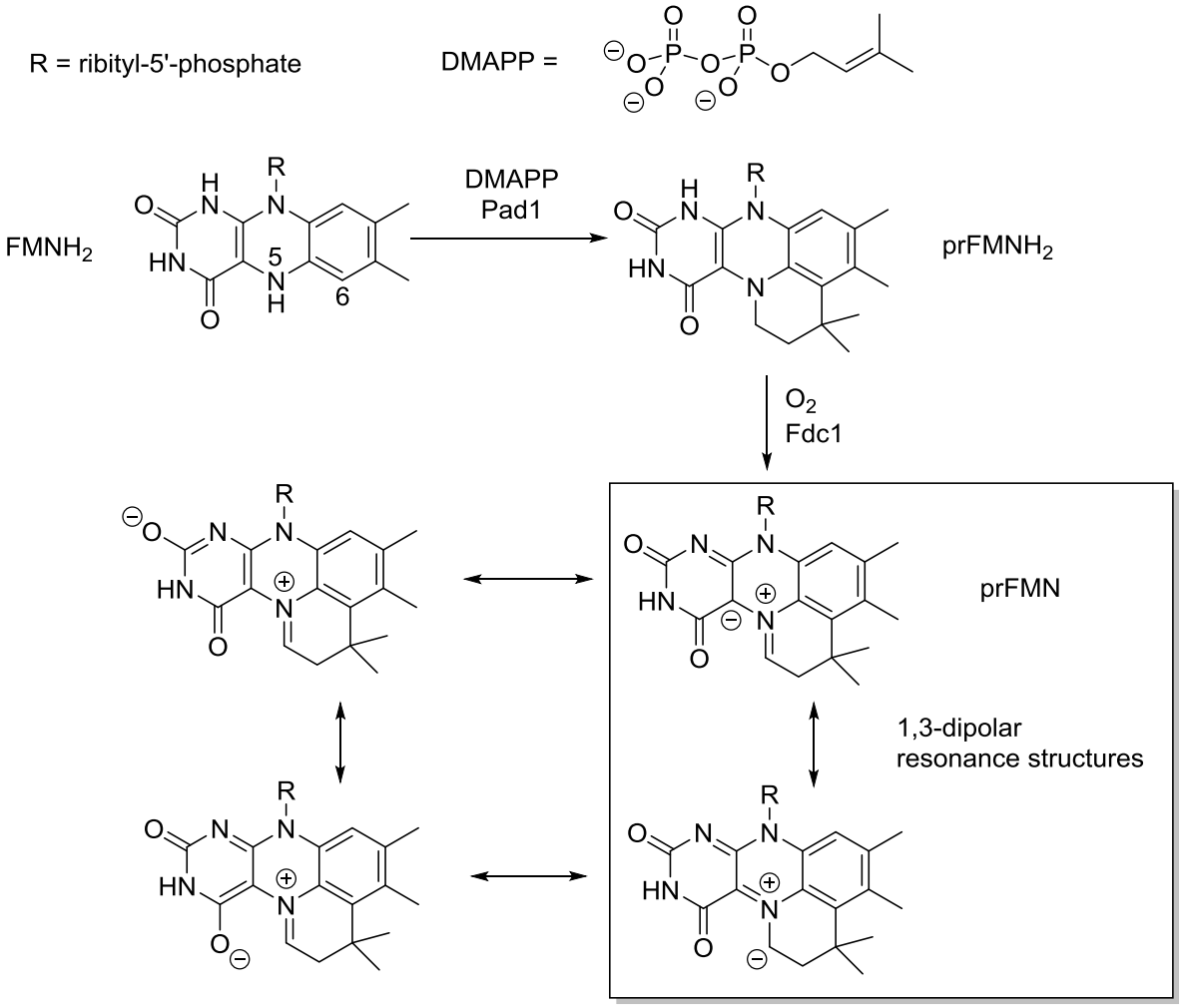

Scheme 2.3. Biosynthesis of prFMN in *S. cerevisiae*.

The dipolar nature of prFMN is a crucial prerequisite for decarboxylase activity, allowing adduct formation *via* 1,3-dipolar cycloaddition with dipolarophilic substrates, such as polyunsaturated carboxylic acids in the case of *S. cerevisiae* Fdc1.

2.4. Overview of 1,3-dipolar cycloaddition chemistry

In general terms, 1,3-dipolar cycloadditions are thermally allowed pericyclic (3+2) reactions resulting in the concerted formation of a five-membered heterocycle from a 1,3-dipole (equivalent to the diene in a Diels-Alder reaction) and a dipolarophile (equivalent to the dienophile). 1,3-Dipoles can be represented as resonance-stabilized zwitterions with two formal charges and four π-electrons distributed across three connected atoms, whereas dipolarophiles are unsaturated

compounds bearing no formal charges, usually alkenes or alkynes. The reaction proceeds in suprafacial manner, with the transition state (TS) forming a cyclic six-electron system with zero nodes, indicating stabilization by Hückel-aromaticity (Scheme 2.4). The thermodynamic driving force behind the reaction can be interpreted as the energetically favorable conversion of two π-bonds into two σ-bonds. Since 1,3-dipoles always contain at least one group V or group VI heteroatom and a large variety of substituted dipolarophiles is commercially available, this reaction is especially useful for the synthesis of five-membered heterocycles, both aromatic and non-aromatic. The equilibrium between reactants and adduct can lie on either side, with the reverse reaction known as retro-cycloaddition, cycloelimination or cycloreversion.[21]

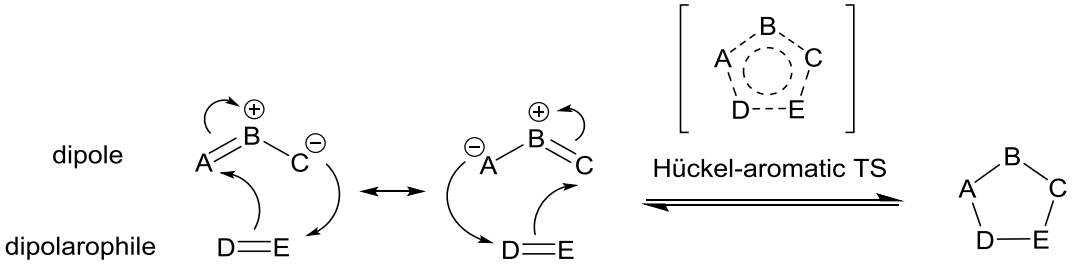

Scheme 2.4. Generalized reaction scheme for 1,3-dipolar cycloaddition.

Azomethine ylides have been characterized as allyl-type (bent-shape) dipoles with pronounced nucleophilic character.[22] Due to their inherent reactivity, they are usually prepared *in situ*, for example by ring-opening of aziridines, followed by immediate reaction with suitable dipolarophiles.[23]

It has been established that cycloadduct formation with nucleophilic nitrogen-centered dipoles is accelerated by electron-withdrawing groups (EWGs) on the dipolarophile by stabilization of the LUMO, whereas electron-donating groups (EDGs) slow down the reaction by raising the dipolarophile's HOMO.[24] The substituents on either dipole or dipolarophile therefore can have great impact on reaction rate and equilibrium.

2.5. Reactivity of prFMN and substrate scope

In the decarboxylation of acrylic acids catalyzed by Fdc1, cycloadduct formation between substrate and cofactor *via* 1,3-dipolar cycloaddition is the first reaction to take place (Scheme 2.5,

steps 1 and 2). After decarboxylative fragmentation (step 3), the accumulation of negative charge at the α-carbon atom is circumvented by delocalization into the cofactor's extended conjugated system, thus stabilizing the transition state. Subsequent protonation by glutamate residue E282 (step 4) promotes cycloelimination (steps 5 and 6), releasing the decarboxylated product and closing the catalytic cycle.[5, 25]

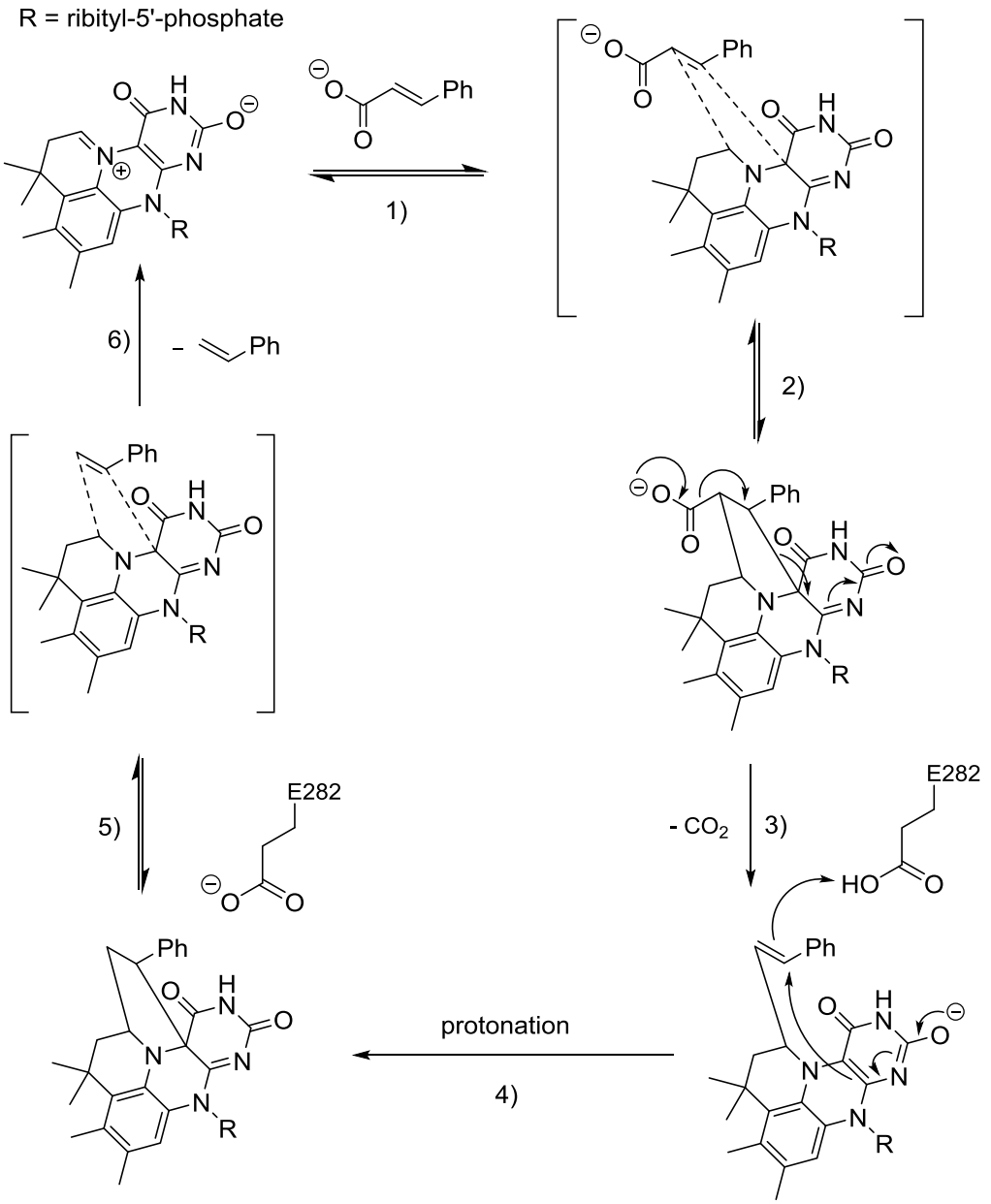

Scheme 2.5. Proposed catalytic cycle of Fdc1.

Concerning the mechanistic aspects of Fdc1, it should be noted that the current literature assumes that the carboxylate anion undergoes cycloaddition followed by decarboxylation, however the experiments performed for this study have shown that optimal conversion was achieved at pH 6, with substantial decarboxylase activity remaining even at pH 3 (see Figure 3.5). At such conditions, weak carboxylic acids exist almost exclusively in their protonated form, suggesting that protonated acid molecules may be able to enter the active site and undergo decarboxylation. Further mechanistic studies are necessary to resolve this discrepancy.

In this study, lyophilized whole cells of *E. coli* containing overexpressed Fdc1 were used as the catalytic system. It was found that this setup was able to effectively decarboxylate a wide variety of acrylic acid derivatives, however not without some limitations. Most importantly, the enzyme only accepted substrates with an extended conjugated π-system (aryl or alkenyl) adjacent to the acrylic acid moiety (see Figure 3.1). This preference is to be expected, since the formation of two new σ-bonds may proceed at different rates, which would produce transient partial charges. Delocalization of these charges into an extended electron system is therefore energetically favored and expected to raise the reaction rate. Additionally, diffuse electron density in both cofactor and substrate molecule allows for more facile initiation of electron flow as well as better matching orbital energies according to principles established by HSAB and FMO approaches.[24, 26]

Due to the intrinsic nucleophilic properties of the azomethine-like cofactor, cycloadduct formation in the reaction mechanism of Fdc1 proceeds primarily through interaction between the HOMO of prFMN and the substrate's LUMO. It can be assumed that potential substrates must show a somewhat ambiguous character: the α,β-unsaturated carboxylic acid molecule must be electrophilic enough to allow adduct formation with the nucleophilic cofactor in the first place, however after decarboxylation and protonation steps, the cycloadduct should dissociate easily into decarboxylation product and cofactor, allowing a new catalytic cycle to initiate. Therefore, it is a reasonable proposition that decarboxylation itself (the loss of one potent EWG as CO_2) is the crucial step that raises electron density in the substrate-cofactor adduct, therefore promoting it to undergo cycloelimination.

Additional EWGs present in the substrate molecule should accelerate the initial cycloaddition, however after decarboxylation, the electron-withdrawing effects would stabilize the cycloadduct and slow down the rate of cycloelimination, potentially even deactivating the enzyme permanently. Strongly electron-deficient dipolarophiles that cannot liberate one of their EWGs through

decarboxylation should therefore be potent mechanistic inhibitors of Fdc1, which has been demonstrated experimentally by Ferguson *et al*. Supplementation of a 10-fold excess of strongly electrophilic 2-fluoro-2-nitrovinylbenzene, which is a good isostere for cinnamic acid, to a preparation of Fdc1 resulted in complete enzyme deactivation (Figure 2.1).[27] The inactive cofactor-inhibitor cycloadduct was identified using UV-Vis spectroscopy and native mass spectrometry. Another mechanistic inhibitor of Fdc1 is 2-hydroxy-3-phenylacrylic acid, which is the enol tautomer of phenylpyruvic acid (Figure 2.1). After decarboxylation, tautomerization of the inhibitor-cofactor adduct occurs, forming an inactive species which is unable to undergo step 4 of the catalytic cycle.[5]

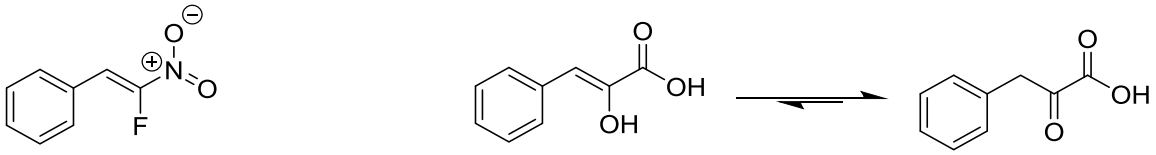

2-fluoro-2-nitrovinylbenzene 2-hydroxy-3-phenylacrylic acid phenylpyruvic acid

Figure 2.1. Mechanistic inhibitors of Fdc1.

2.6. Potential applications of Fdc1

Currently, industrially important light alkenes such as ethylene, propylene and butadiene are produced primarily by catalytic steam cracking of crude oil fractions, which has been described as the single most energy-demanding process in the petrochemical industry.[28] Styrene, on the other hand, is prepared on a large scale by catalytic dehydrogenation of petroleum-derived ethylbenzene.[29] The investigation of more energy-efficient synthetic routes towards these compounds is therefore highly desirable both from ecological and economical viewpoints. Biocatalytic systems might provide alternatives that are environmentally benign and function under mild conditions.

The successful *de novo* biosynthesis of styrene from renewable sugars by metabolically engineered, phenylalanine-overproducing strains of *E. coli* and *S. cerevisiae* has been reported by McKenna *et al.*, utilizing phenylalanine ammonia lyase (Pal2) from *Arabidopsis thaliana* as well as Fdc1 from *S. cerevisiae* (Scheme 2.7).[30]

This approach is particularly interesting since it exploits the active metabolism of living cells. The

necessity for elaborate protein isolation was eliminated and styrene production could be initiated simply by cultivating the manipulated strains in the presence of glucose. In the *E. coli* strain, styrene titers reached as far as 260 mg/L, approaching the toxicity threshold of approx. 300 mg/L.

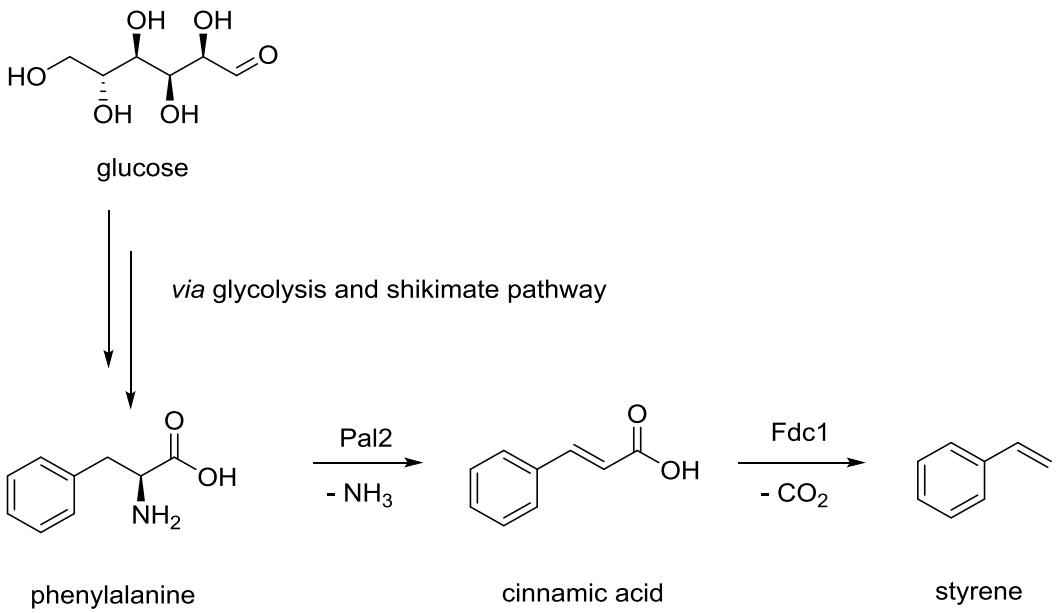

Scheme 2.7. Styrene production from glucose by recombinant *E. coli* or *S. cerevisiae*.

These findings as well as the unusual nature of the protein's cofactor clearly show the synthetic potential of Fdc1. Therefore, a characterization of the protein in respect to fundamental parameters such as temperature stability, pH optimum and substrate scope is a logical next step in the investigation of this enzyme.

Furthermore, Fdc1 has not yet been subjected to detailed studies of its ability to catalyze the β-carboxylation of styrenes and other terminal alkenes. Currently, the established enzyme toolbox for this reaction (which is not feasible with traditional chemical methods) mechanistically requires an activating *para*-hydroxy group on the substrate molecule, a prerequisite that severely limits the applicability of those systems.[14c-e] The reaction mechanism of Fdc1 does not imply the strict necessity for such a feature. Whereas no carboxylation could be achieved in the experiments performed for this study, further research on this topic might produce a synthetic platform with substantial uses for the regioselective functionalization of unsaturated molecules.

3. Results and Discussion

3.1. Protein expression

To elucidate the potential applications of Fdc1, the enzyme was overexpressed in chemically competent BL21(DE3) *E. coli* host cells. The initial strain was transformed by heat shock with a pET21b vector containing *S. cerevisiae fdc1* and *E. coli ubiX* at NdeI and XhoI sites.[5] UbiX was co-expressed to ensure a sufficient amount of prenylated flavin *in vivo*. Protein expression was induced with 330 µM IPTG. Additionally, 12 µM $MnCl_2$ were supplemented since cofactor binding in Fdc1 is mediated by the phosphate group on the ribityl sidechain and depends on K^+ as well as Mn^{2+}.[5] After lyophilization of the cultivated cells, expression of the desired protein was confirmed for each batch by SDS-PAGE analysis (see Figure S1, approx. 56 kDa) and a subsequent test for decarboxylase activity with 10 mM ferulic acid. For standard reaction conditions, see Figure 3.1.

Due to concerns about the stability of protein and cofactor, the lyophilized cells were stored at 4 °C under a protective argon atmosphere to prevent deactivation by moisture or oxygen. This strategy proved to be successful, since no observable loss of activity was detected after multiple weeks of storage.

3.2. Substrate scope

37 structurally diverse α,β-unsaturated carboxylic acids were tested in the decarboxylation direction by supplementing them at a concentration of 10 mM to rehydrated cells (Figures 3.1 and 3.2). The obtained results show a clear trend that Fdc1 readily decarboxylates substrates with an extended conjugated π-electron system adjacent to an acrylic acid moiety, whereas substrates with only a single α,β-C=C bond were not accepted.

Fdc1 was able to completely decarboxylate (> 99% conv.) the majority of accepted substrates (**1a** – **3a**, **7a**, **12a** – **18a** and **20a**) under standard conditions, including heterocyclic compounds (**9a** and **10a**). Concerning aryl-substituted substrates, the enzyme tolerated a large variety of substituents (methyl, methoxy, hydroxy, halide and amino groups) on the aromatic substructure, however increasing steric hindrance in *ortho*-position to the acrylic acid moiety slowed down the reaction, resulting in incomplete turnover of **5a** and **6a** (31 – 36% conv.), whereas their structural isomer **7a** was fully converted (> 99% conv.). Steric hindrance is also obvious for the bulky *para*-

phenoxy group in **35**. This pattern clearly indicates that molecule geometry and size is a major factor in the substrate preference of Fdc1. Furthermore, we observed that **4a**, **11a** and **19a** gave incomplete conversions (9 – 86% conv.), while **33** was rejected entirely (< 1% conv.), implying that EDGs diminish the reaction rate. Imidazole-derivatives **31** and **32** are predominantly protonated at pH 6.0 and therefore positively charged, which might have been a factor for their rejection. Thiophene-2-carboxylic acid (**26**) was not converted, likely due to the high energetic barrier of transient dearomatization and the lack of a dipolarophilic C=C bond.

These findings can be explained with the inherent nucleophilic properties of the enzyme's azomethine-like cofactor, which disfavors adduct formation with electron-rich dipolarophiles (see section 2.5). Additionally, it can be assumed that mass transfer limitations of polar molecules across the bacterial cell membrane of the whole-cell catalyst as well as hydrogen-bonding interactions in the active site influence substrate preference by a large margin.

Phenylpropiolic acid (**30**) is a rather puzzling non-substrate, since it is the sp-hybridized analog to cinnamic acid (**14a**). At the current moment, there can be no clear delineation if the rejection of **30** was caused primarily by electronic effects or by steric limitations.

The obtained results suggest a clear pattern of structural and electronic requirements for substrates to be accepted by Fdc1:

a) The substrate must be equipped with an acrylic acid moiety substituted with an extended conjugated π-system at C3, which can either consist of an aromatic ring or at least one further C=C bond.
b) Compounds lacking an α,β-C=C bond are principally unable to undergo cycloaddition with the cofactor and are therefore unreactive.
c) The *cis*/*trans*-configuration of the acrylic double bond appears to be critical, with a preference for *cis* isomers.
d) Sterically demanding and/or strongly electron-donating groups tend to impede the reaction.
e) Substrates bearing a carboxylate group directly attached to an aromatic system are unable to undergo cycloaddition with the cofactor and are therefore unreactive.

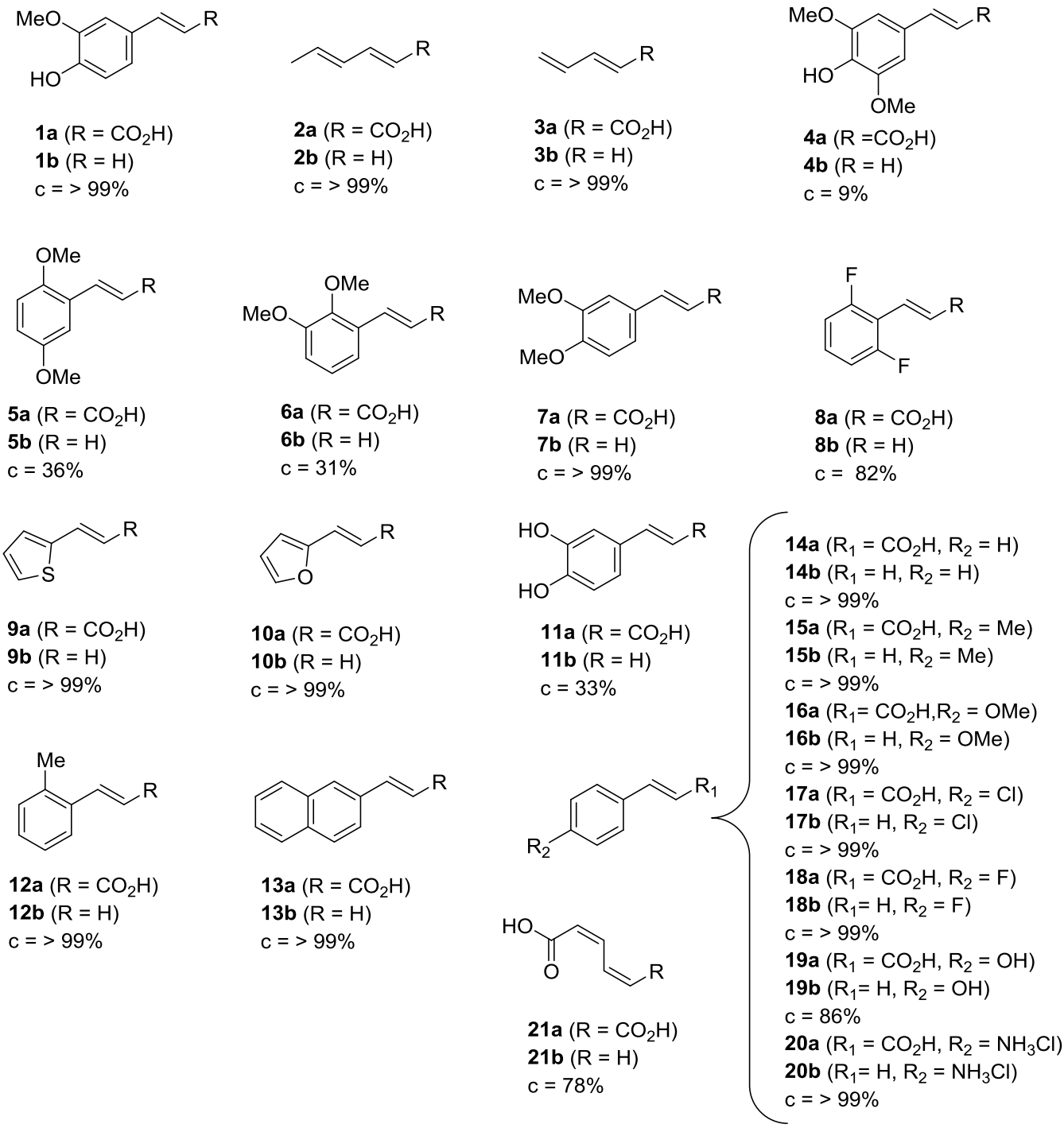

Figure 3.1. Substrates accepted by Fdc1 (**1** – **21a**) and their corresponding products (**1** – **21b**, c = conversion). [a] Reaction conditions: phosphate buffer (100 mM, pH 6.0), whole lyophilized cells of *E. coli* containing Fdc1 (30 mg/mL), 10 mM substrate, 30 °C, 120 rpm, 18 h, 5% v/v DMSO (20% v/v DMSO for **13a**). [b] Conversions were determined by calibrated reversed-phase HPLC.

The successful decarboxylation of non-aromatics **2a** and **3a** led us to investigate the possibility to convert muconic acid, which is of substantial industrial relevance as a precursor of adipic acid, which in turn is required in large quantities in the production of nylon.[31] The biosynthesis of muconic acid in *S. cerevisiae* has been reported, so both *trans,trans*-muconic acid (**27**) and *cis,cis*-muconic acid (**21a**) were included in the screening procedures.[32] Interestingly, **27** does fulfill the selection criteria outlined above and has similar structural properties as **2a** and **3a**, yet was not converted by Fdc1. This might indicate that a certain degree of polarization in the acrylic double bond is necessary to allow formation of the substrate-cofactor adduct, a feature that is not present in **27** due to its symmetry. **21a**, however, was partially converted, but it should be noted that this species is rather unstable due to its unfavorable double bond conformations and is expected to show higher reactivity, thus other ways of decomposition must also be considered.

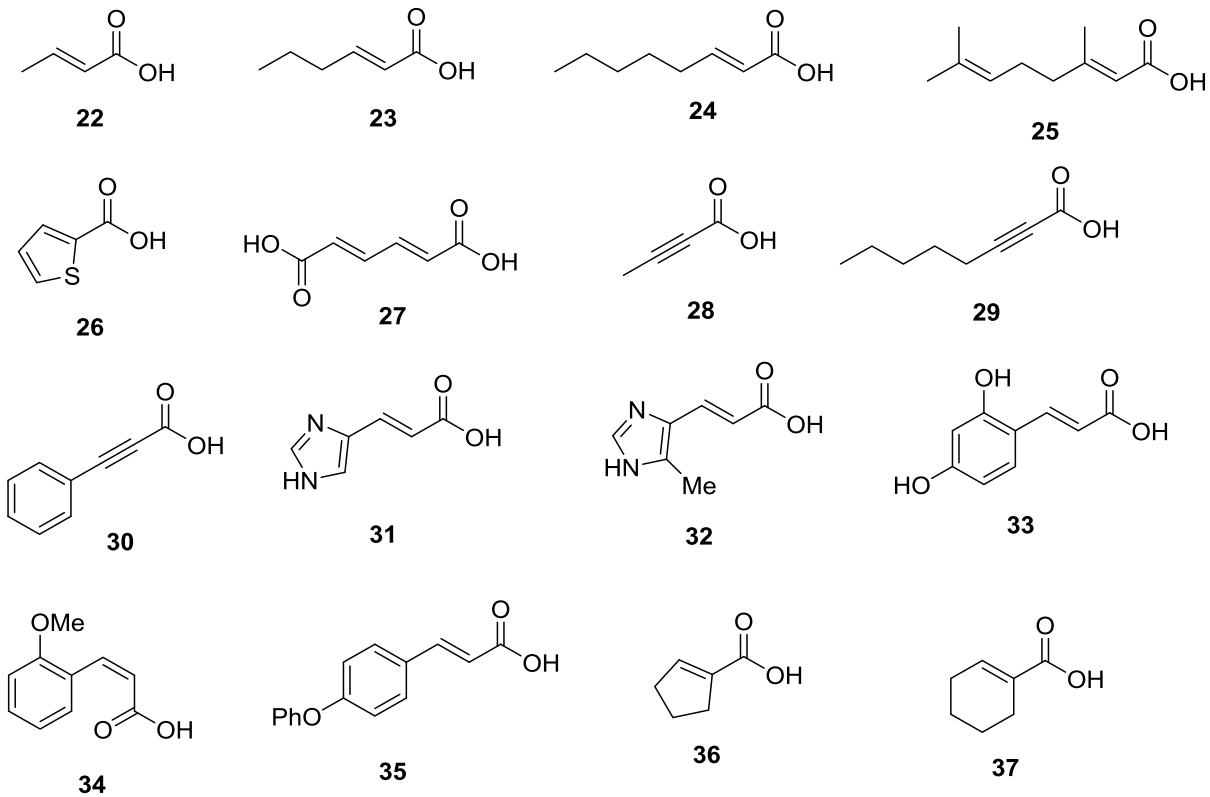

Figure 3.2. Non-substrates rejected by Fdc1 (all conversions < 1%). [a] Reaction conditions: phosphate buffer (100 mM, pH 6.0), whole lyophilized cells of *E. coli* containing Fdc1 (30 mg/mL), 10 mM substrate, 30 °C, 120 rpm, 18 h, 5% v/v DMSO (20% v/v DMSO for **35**). [b] Analysis was performed with reversed-phase HPLC or GC-MS headspace sampling.

3.3. Carboxylation experiments with $KHCO_3$ or CO_2

As a model substrate for the carboxylation attempts, **1b** was chosen due to its reasonable solubility in aqueous buffer compared to other styrene species. Using varying amounts of catalyst (30 – 50 mg/mL lyophilized cells), $KHCO_3$ (0.5 – 3 M) as C_1 donor and DMSO (5 – 20% v/v) as solubilizer, no formation of the desired product **1a** was observed. Using large catalyst loads (100 mg/mL) and applying pressurized CO_2 (30 bar) for 18 h did produce a minor amount of **1a**, however conversions were below 1%. This should be seen as a proof of principle that carboxylation of alkenes with Fdc1 is feasible to at least a very small extent, but also that further research is necessary to explore the possibility of practical product yields.

Additionally, it must be noted that **1b** partially decomposed when exposed to the aqueous, aerobic conditions used in these experiments, indicated by the formation of a colorless, unidentified precipitate in our control blanks containing no lyophilized cells. Dimerization of the structurally related 4-vinylphenol (**19b**) has been reported, suggesting a similar way of decomposition in our assays.[33] Prevention of this undesired degradation is of utmost importance to ensure acceptable reproducibility and productivity, but this problem could not be solved in a satisfying fashion as of now. Using 1,3-pentadiene (**2b**), isoprene (**38**) or myrcene (**39**) instead of **1b** did not result in any formation of carboxylated product using $KHCO_3$ (Figure 3.3), likely due to unfavorable reaction thermodynamics and the immiscibility of these compounds with the aqueous layer, even when supplementing 20% v/v DMSO or DME as solubilizer.

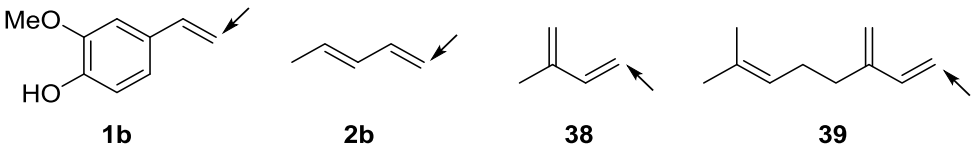

Figure 3.3. Substrates tested in the carboxylation direction with Fdc1 (all conversions < 1%). The arrow points to the expected site of carboxylation. [a] Reaction conditions for assays with $KHCO_3$: phosphate buffer (100 mM, pH 5.5), whole lyophilized cells of *E. coli* containing Fdc1 (30 – 50 mg/mL), 10 mM substrate, $KHCO_3$ (0.5 – 3 M), 30 °C, 120 rpm, 18 – 20 h, 5 – 20% v/v DMSO or DME. [b] Reaction conditions using pressurized CO_2: phosphate buffer (250 mM, pH 7.5), whole lyophilized cells of *E. coli* containing Fdc1 (100 mg/mL), 10 mM substrate (**1b** only), pressurized CO_2 (30 bar), 30 °C, 50 rpm, 18 h, 5% v/v DMSO. [c] Conversions were determined by calibrated reversed-phase HPLC.

3.4. Reaction time

Investigation of reaction time revealed that the decarboxylation of 10 mM **1a** or **2a** reached completion after approx. 16 h (Figure 3.4). The decline in concentration followed a hyperbolic curve, with little difference between the two tested substrates. **1b** concentrations produced from **1a** peaked at 5.4 mM, which is well below the expected concentration of 10 mM. This deviation likely occurred because of product decomposition, as mentioned above.

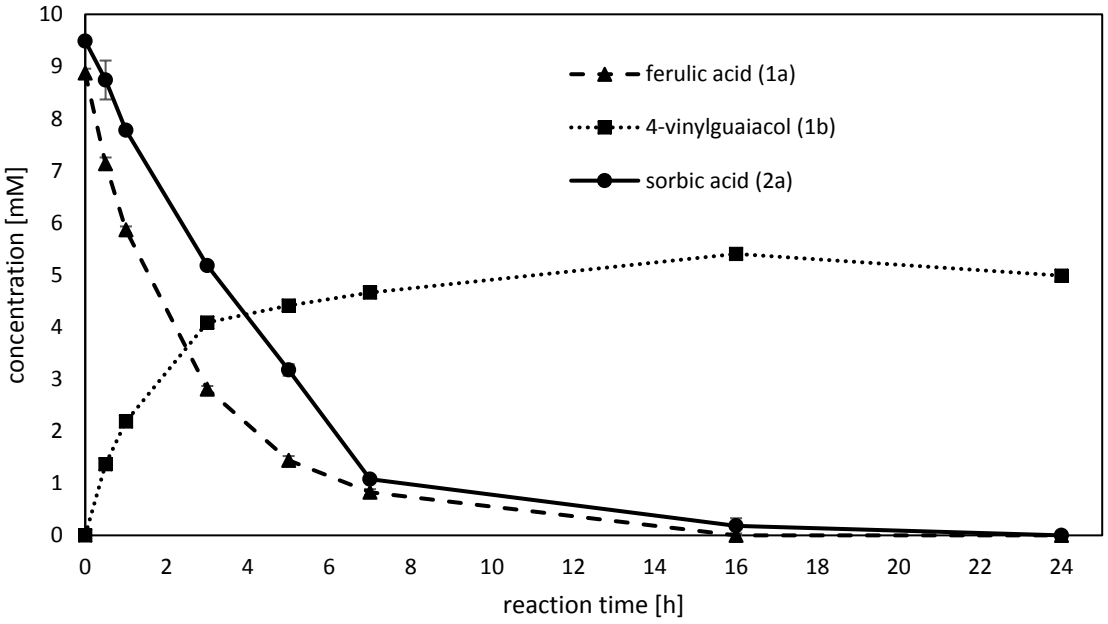

Figure 3.4. Decarboxylation of ferulic acid (**1a**) and sorbic acid (**2a**) over time. [a] Reaction conditions: phosphate buffer (100 mM, pH 6.0), whole lyophilized cells of *E. coli* containing Fdc1 (30 mg/mL), 10 mM substrate, 30 °C, 120 rpm, 5% v/v DMSO; 0.5 – 24 h (data points at 0 h are the results of blanks containing no cells). [b] Conversions were determined by calibrated reversed-phase HPLC.

3.5. Reaction pH

Conversion of **1a** to **1b** depended on pH in a bell-shaped pattern peaking at pH 6.0, whereas conversion of **2a** to **2b** reached completion even at pH 3.0 (Figure 3.5). At these conditions, weak carboxylic acids like the ones used in this experiment should exist almost exclusively in their protonated form, indicating that protonated substrate may enter the active site and undergo

decarboxylation, contrasting previously published mechanistic considerations that assumed the carboxylate anion to undergo adduct formation followed by decarboxylation. Lower conversions at neutral to basic pH were likely caused by hydroxide-induced decomposition of the enzyme or its cofactor.

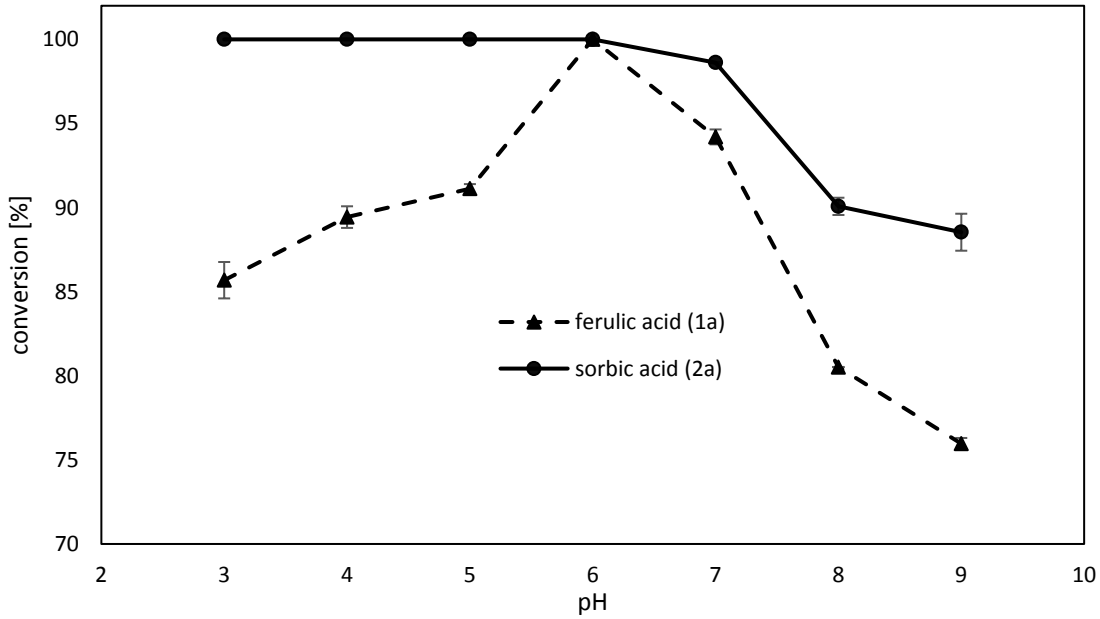

Figure 3.5. Decarboxylation of ferulic acid (**1a**) and sorbic acid (**2a**) against pH. [a] Reaction conditions: phosphate buffer (100 mM, pH 3.0 – 9.0), whole lyophilized cells of *E. coli* containing Fdc1 (30 mg/mL), 10 mM substrate, 30 °C, 120 rpm, 18 h, 5% v/v DMSO. [b] Conversions were determined by calibrated reversed-phase HPLC.

3.6. Reaction temperature

It was found that Fdc1 operates optimally at a temperature range between 30 – 45 °C (Figure 3.6). At 20 °C conversion was incomplete presumably due to diminished reaction rates whereas above 45 °C conversions dropped sharply with rising temperatures, likely due to deactivation of the enzyme.

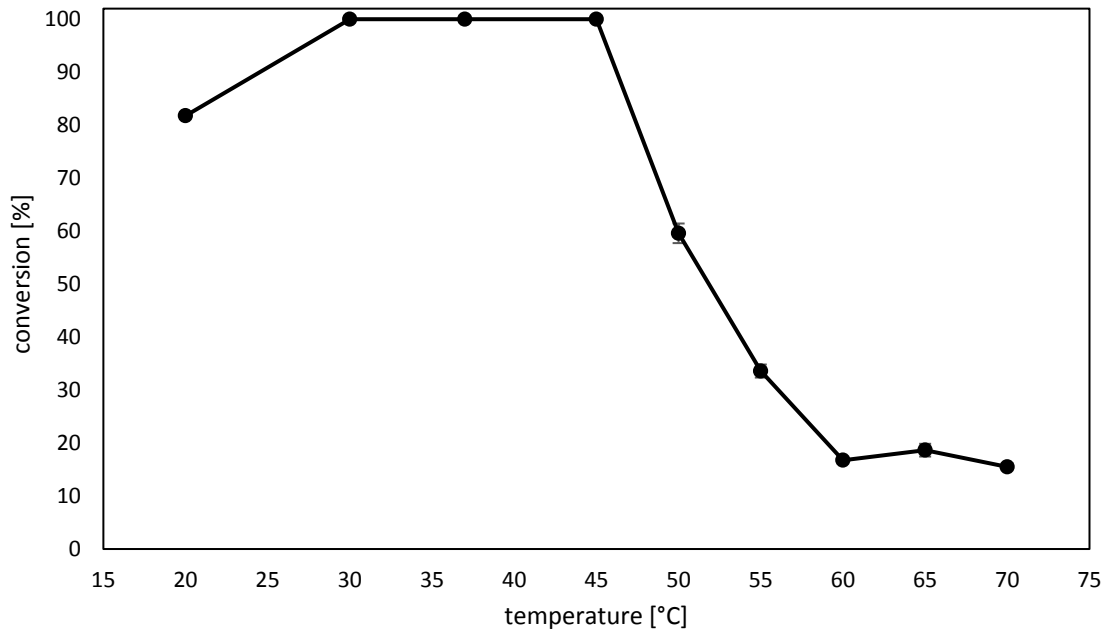

Figure 3.6. Conversion of sorbic acid (**2a**) against temperature. [a] Reaction conditions: phosphate buffer (100 mM, pH 6.0), whole lyophilized cells of *E. coli* containing Fdc1 (30 mg/mL), 10 mM substrate, 20 – 70 °C, 120 or 300 rpm, 18 h, 5% v/v DMSO. [b] Conversions were determined by calibrated reversed-phase HPLC.

3.7. Co-solvents

To test the compatibility of Fdc1 with organic co-solvents, 14 commonly used laboratory solvents were supplemented at concentrations of 5%, 10% and 20% v/v (Figure 3.7). Water-miscible solvents were tolerated quite well, usually showing negligible to small impact at 5% v/v, with some examples, such as MeOH, EtOH, DME, DMF and DMSO, producing viable results at even higher amounts. This greatly expands the protein's applicability, since the use of organic solvents as solubilizers facilitates the conversion of substrates with limited solubility in aqueous buffer. However, all tested immiscible solvents obliterated activity almost completely even at low amounts, showing that the protein is not well suited to the presence of an apolar second phase.

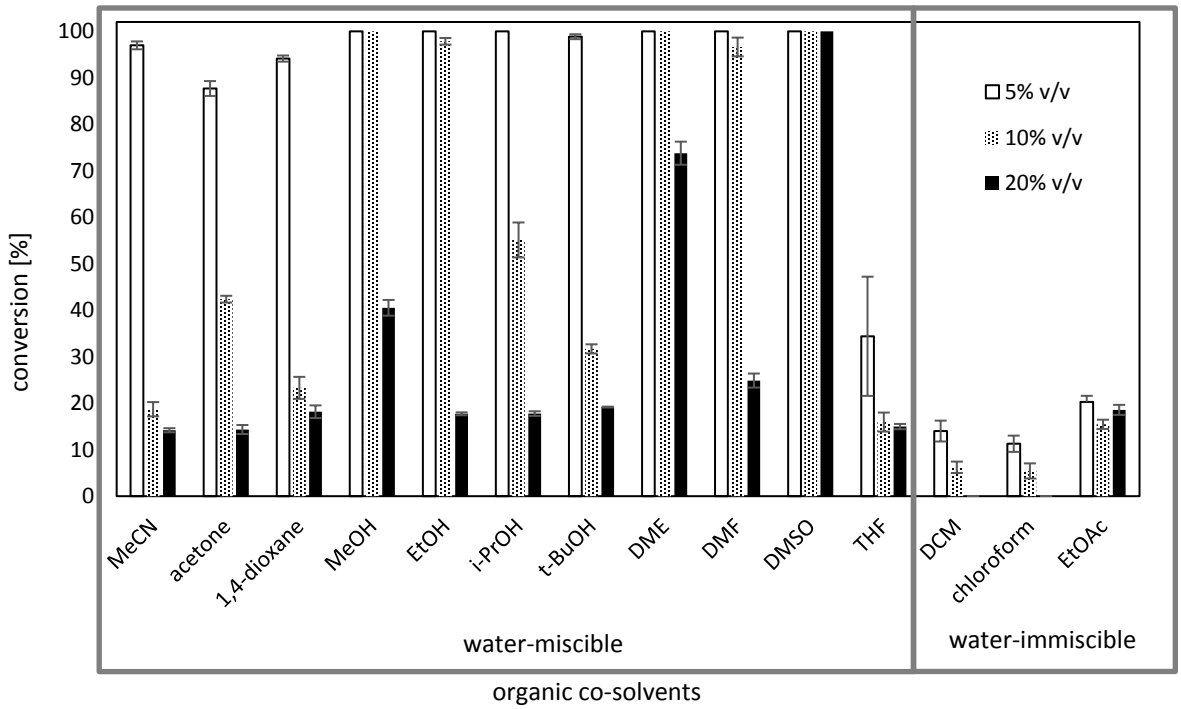

Figure 3.7. Conversion of sorbic acid (**2a**) in the presence of organic solvents. [a] Reaction conditions: phosphate buffer (100 mM, pH 6.0), whole lyophilized cells of *E. coli* containing Fdc1 (30 mg/mL), 10 mM substrate, organic co-solvents (5 – 20% v/v), 30 °C, 120 rpm, 18 h. [b] Conversions were determined by calibrated reversed-phase HPLC.

3.8. Upscaling

Conclusively, a preparative-scale biotransformation of **1a** to **1b** was performed. Substrate load was increased from 10 mM to 16.8 mM (65.1 mg **1a** in 20 mL solution) and reaction time was prolonged from 18 h to 24 h. To prevent radical-induced product decomposition, 10 wt% of the radical scavenger hydroquinone (6.5 mg) was added to the reaction mixture. After scheduled reaction time, solid parts of the reaction mixture were separated by centrifugation. Subsequent HPLC-DAD analysis of the supernatant revealed incomplete turnover of the starting material (8.7 mM of unreacted **1a** remained, 48% conversion). The desired product was isolated by manual extraction of the supernatant with EtOAc and purification by flash column chromatography (silica, DCM), giving 19 mg (38% yield) of **1b**. Product identity and purity were confirmed by ^{1}H and ^{13}C NMR spectroscopy. Extending the reaction time or increasing catalyst load are expected to be effective strategies to solve the problem of incomplete substrate turnover.

4. Conclusion

In this study, fungal decarboxylase Fdc1 was characterized successfully in regard to substrate scope, reaction time, pH optimum, temperature optimum and compatibility with organic co-solvents. The enzyme is able to decarboxylate a diverse set of polyunsaturated carboxylic acids, as long as some essential criteria for substrate properties are fulfilled.

The performed carboxylation experiments were largely unsuccessful. Further research is required to elucidate the enzyme's practicality in the thermodynamically disfavored carboxylation direction.

For possible future applications regarding the production of bulk and fine chemicals, the inherent problem of product stability must be challenged to ensure acceptable yields that can reliably be accomplished.

Acknowledgment

We would like to thank the research group of Prof. David Leys (University of Manchester) for sharing their knowledge and providing us with the genetic material encoding for Fdc1.

5. Experimental Procedures

Transformation and preparation of glycerol stocks: 3 µL of vector preparation (pET21b containing *S. cerevisiae fdc1* and *E. coli ubiX* at NdeI and XhoI sites) was added to 100 µL chemically competent BL21(DE3) *E. coli* cells. The mixture was cooled with an icebath for 30 min, then heated to 42 °C for 15 s. 900 µL LB medium was added and the mixture was shaken at 37 °C and 300 rpm for 1 h. 100 µL of the cell suspension was spread onto LB-agar plates supplemented with 100 µg/mL ampicillin and grown at 30 °C overnight. The next day, a single culture was picked and used to inoculate 10 mL of LB medium (100 µg/mL ampicillin), followed by overnight cultivation at 30 °C and 120 rpm. 20 glycerol stocks were prepared by adding 500 µL of aqueous glycerol solution (30%) to 500 µL of culture medium. The stocks were stored at -20 °C until needed.

General procedure for protein expression: seed cultures were prepared by inoculating 10 mL of LB medium with glycerol stock, addition of 100 µg/mL ampicillin and incubation at 30 °C and 120 rpm overnight. The next day, 3 × 1 L of autoclaved LB medium was supplemented with 100 mg/L ampicillin and 10 mL of seed culture each. Cells were grown at 37 °C and 140 rpm until an OD_{600} between 0.6 and 0.8 was observed (approx. 2.5 h), followed by induction with 330 µM IPTG and 12 µM $MnCl_2$. Cultures were shaken overnight at 15 – 18 °C and 140 rpm. The following day, the cells were separated from the medium by centrifugation at 4 °C and 4000 rpm for 20 min and resuspended in wash buffer (50 mM phosphate, pH 7.5). The stems were united and centrifuged again. The cell pellet was flash frozen in liquid N_2, followed by overnight lyophilization. The lyophilized cells were stored until needed at 4 °C under a protective argon atmosphere to prevent enzyme deactivation by oxidation or hydrolysis.

Expression of the desired protein was controlled by SDS-PAGE analysis as well as decarboxylation assays containing 10 mM **1a**. For SDS-PAGE, 10 mg of lyophilized cells were rehydrated in 1 mL of distilled water for 30 min at 30 °C and 120 rpm and centrifuged for 10 min at 14000 rpm. The supernatant was separated and the solids were resuspended in 700 µL of 6 M aqueous urea solution. 30 µL of supernatant and 30 µL of pellet suspension were each supplemented with 30 µL of commercial Laemmli sample buffer and heated to 95 °C for 5 min at 700 rpm. Separation was performed in Genscript ExpressPlus PAGE polyacrylamide gel with

ThermoFisher prestained PageRuler protein ladder as mass standard, in Tris-MOPS buffer at 100 V until the dye front reached the bottom of the gel. The gel was stained with Coomassie-Blue overnight and then destained with distilled water.

General procedure for decarboxylation: assays were prepared by filling 30 mg lyophilized whole cells containing overexpressed Fdc1 into 1.5 mL plastic Eppendorf tubes, addition of 950 µL phosphate buffer (100 mM, pH 6.0) and rehydration for 30 min at 30 °C and 120 rpm. Substrates were supplied to the mixture by adding 50 µL of 200 mM stock solutions in DMSO to achieve reaction volumes of 1 mL and substrate concentrations of 10 mM, followed by incubation for 18 h at 30 °C and 120 rpm in horizontal position under exclusion of ambient light. After scheduled reaction time, samples were centrifuged at 14000 rpm for 10 min and 100 µL of supernatant was diluted with 900 µL of H_2O/MeCN/trifluoroacetic acid (TFA, 50:50:3) to precipitate residual protein. The diluted sample was centrifuged again, followed by analysis with HPLC-DAD. All reactions were performed in triplicate plus one control blank without lyophilized cells.

Substrate scope: a stock solution of the substrate of interest was added to rehydrated cells, followed by incubation. For substrates showing limited solubility (**13a**, **35**), lyophilized cells were suspended in 800 µL of buffer and after rehydration, 150 µL of pure DMSO was supplemented, followed by addition of 50 µL substrate stock and incubation.

Reaction time: a stock solution of either **1a** or **2a** was added to rehydrated cells, followed by incubation for scheduled timespans (0.5 – 24 h). For data points representing 0 h reaction time, control blanks containing no lyophilized cells were used.

Reaction pH: lyophilized cells were suspended in the corresponding phosphate buffer (100 mM, pH 3.0 – 9.0) and rehydrated. A stock solution of either **1a** or **2a** was added to the mixture and incubated.

Reaction temperature: a stock solution of **2a** was added to rehydrated cells. The tubes were placed in pre-tempered thermo-shakers and shaken in horizontal position at either 120 rpm (20 – 37 °C) or 300 rpm (45 – 70 °C).

Screening of co-solvents: 200 mM stock solutions of **2a** were prepared in MeCN, acetone, 1,4-dioxane, MeOH, EtOH, *i*-PrOH, *t*-BuOH, DME, DMF, DMSO, THF, DCM, chloroform and EtOAc. Lyophilized cells were suspended in 800, 900 or 950 µL of phosphate buffer (100 mM, pH 6.0) and rehydrated. 50 µL of the corresponding stock solution was added to the mixture, followed by addition of pure co-solvent to achieve reaction volumes of 1 mL and subsequent incubation. For water-miscible co-solvents, sample preparation was described as above. For immiscible solvents, partial evaporation of the organic layer was observed and therefore, only the aqueous phases were analyzed using HPLC-DAD.

General procedure for carboxylation using $KHCO_3$: 30 – 50 mg lyophilized cells were suspended in 800 – 950 µL phosphate buffer (100 mM, pH 5.5) and rehydrated. Pure co-solvent (0 – 150 µL) followed by 50 µL substrate stock (**1b**, **2b** and **38** 200 mM in DMSO or **39** 200 mM in DME) was added to achieve reaction volumes of 1 mL, followed by transfer of the mixture into a screw-neck glass vial containing 50 – 300 mg (0.5 – 3 M) $KHCO_3$. The vessels were swiftly closed to avoid the loss of emerging CO_2 gas and incubated for 18 – 20 h.

General procedure for carboxylation using pressurized CO_2: 300 mg of lyophilized cells were suspended in 2850 µL phosphate buffer (250 mM, pH 7.5) and rehydrated. A higher buffer strength was chosen to counterbalance a sharp drop in pH caused by the large CO_2 load. 150 µL of a 200 mM stock solution of **1b** in DMSO was added and the mixture was transferred into a steel pressure vessel equipped with a stir bar. The reaction mixture was pressurized with technical CO_2 gas (30 bar) and stirred at 50 rpm and 30 °C for 18 h.

Preparative-scale decarboxylation of **1a**: 560 mg lyophilized cells were filled into a 50 mL plastic vial, suspended in 19 mL phosphate buffer (100 mM, pH 6.0) and rehydrated. 65.1 mg (0.34 mmol) of **1a** and 6.5 mg (0.06 mmol) of hydroquinone was dissolved in 1 mL of MeOH and added to the mixture. The vessel was wrapped in aluminum foil to ensure protection from ambient light and incubated for 24 h at 120 rpm and 30 °C. Solids were separated by centrifugation at 4000 rpm and 4 °C for 20 min. 100 µL of supernatant was diluted with H_2O/MeCN/TFA and subjected to HPLC-DAD analysis, which revealed incomplete turnover of the starting material (48% conversion). The

remaining liquid was extracted with EtOAc (4 × 20 mL). The organic phase was united, dried with Na_2SO_4 and filtered. After evaporation of the filter solution, a mixture of off-white solids and dark yellow oil was obtained. The oil was diluted with DCM and purified by flash column chromatography (silica, DCM), giving 19 mg (0.13 mmol, 38% yield) of spectroscopically pure **1b** as a colorless oil with a distinct clove-like odor. A prominent water peak at 3.55 ppm was likely caused by contamination of the hygroscopic solvent DMSO-d_6 (see Figures S2 and S3).

1b: ^{1}H NMR (300 MHz, DMSO-d_6): δ = 9.09 (s, 1H), 7.04 (d, *J* = 1.9 Hz, 1H), 6.85 (dd, *J* = 8.1, 1.9 Hz, 1H), 6.72 (d, *J* = 8.1 Hz, 1H), 6.60 (dd, *J* = 17.6, 10.9 Hz, 1H), 5.63 (dd, *J* = 17.6, 1.1 Hz, 1H), 5.05 (dd, *J* = 10.9, 1.0 Hz, 1H), 3.78 (s, 3H); ^{13}C NMR (75 MHz, DMSO-d_6): δ = 147.69, 146.71, 136.71, 128.79, 119.53, 115.36, 110.95, 109.57, 55.56.[34]

General procedure for HPLC-DAD analysis: samples were analyzed on an Agilent Infinity 1260 HPLC-DAD setup equipped with a reversed-phase Phenomenex Luna C18 column (250 × 4.6 mm). The mobile phase was composed of H_2O (0.1% v/v TFA) and a MeCN (0.1% v/v TFA) gradient with the following amounts of MeCN: 0 – 2 min 5%; 2 – 15 min 5 – 100%; 15 – 17 min 100%; 17 – 22 min 100 – 5%. The instrument was calibrated with authentic reference materials and the reduction of substrate peaks and emerging of product peaks absent in the control blanks was monitored. Due to the instability of the decarboxylation products, conversions were determined indirectly through the reduction of substrate peaks.

General procedure for GC-MS headspace analysis: to qualitatively verify the formation of volatile decarboxylation products not detectable on the used HPLC-DAD setup, reactions were performed in glass vials capped with rubber septa and analyzed directly with an Agilent 7697A headspace sampler (oven temperature: 80 °C; loop temperature: 90 °C; transfer line temperature: 100 °C; vial equilibration time: 2 min; vial pressurization: 15 psi, pressurization gas: helium) connected to an Agilent 7890A GC machine (oven temperature: 50 °C; column: Agilent J&W HP-5ms capillary column (30 m × 0.25 mm × 0.25 µm; stationary phase: bonded & cross-linked 5%-phenyl-methylpolysiloxane) coupled to an Agilent 5975C mass-selective detector (electron impact ionisation, 70 eV; quadrupole mass selection) using helium as carrier gas.

Supporting Information

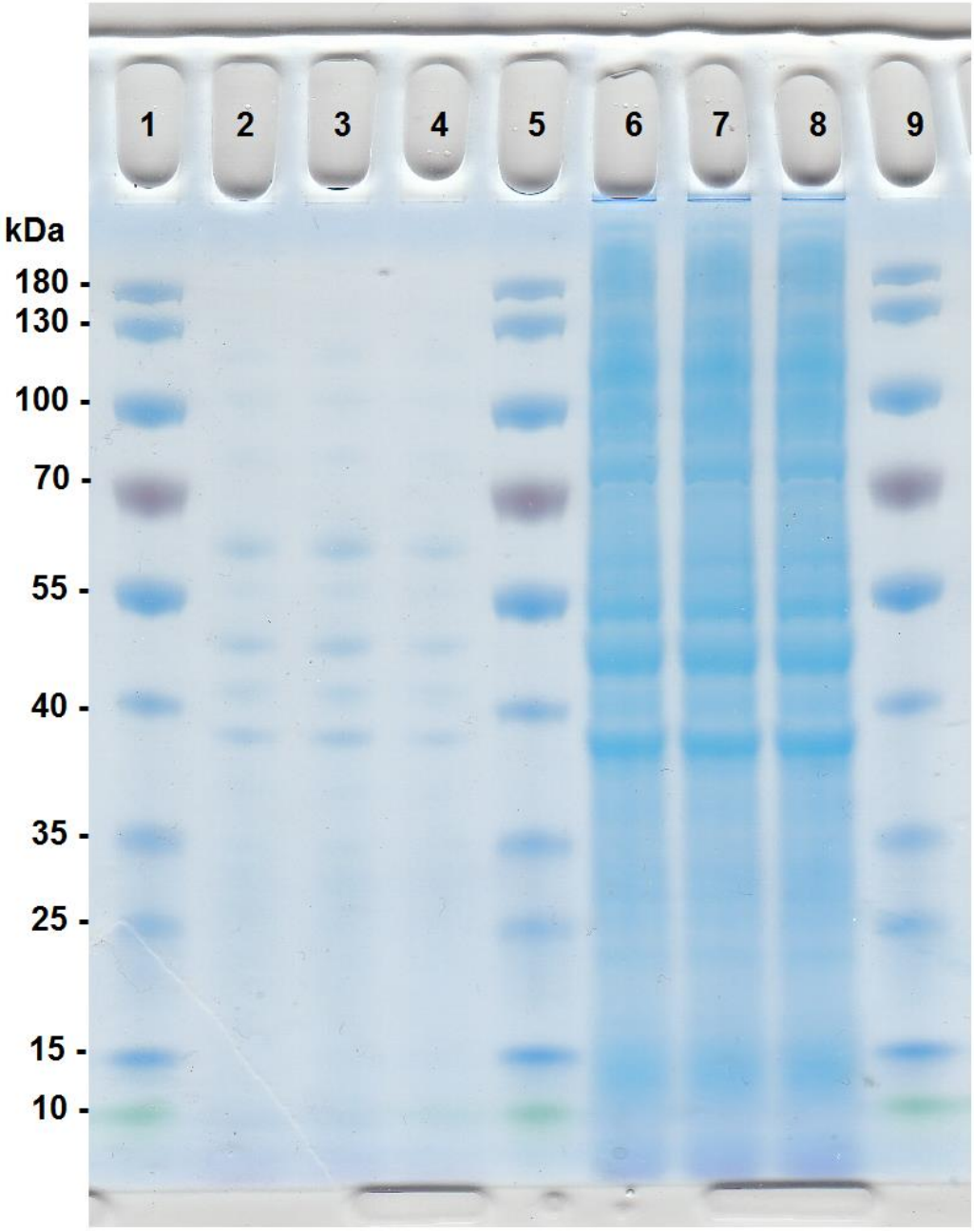

Figure S1. Representative SDS-PAGE of cultivated cells overexpressing Fdc1. Wells 1, 5, 9: PageRuler protein standard, Wells 2 – 4: supernatant, Wells 6 – 8: resuspended cell pellet.

Table S1. HPLC-DAD retention times and detection wavelengths (n.d. = not detected).

compound	retention time [min]	detection wavelength [nm]
1a/b	10.8/13.3	310/263
2a/b	11.6/15.7	263/263
3a/b	10.4/n.d.	254/n.d.
4a/b	10.7/12.9	310/220
5a/b	12.8/15.5	280/220
6a/b	12.5/15.3	280/220
7a/b	11.8/14.5	310/263
8a/b	13.0/16.4	263/254
9a/b	12.2/15.5	310/280
10a/b	11.4/14.5	310/263
11a/b	9.8/12.0	310/263
12a/b	13.2/16.5	280/254
13a/b	14.2/17.2	263/254
14a/b	12.6/15.9	280/254
15a/b	13.4/16.8	280/254
16a/b	12.6/15.7	310/263
17a/b	13.7/16.9	280/254
18a/b	12.8/15.8	280/254
19a/b	10.7/13.2	310/263
20a/b	7.5/9.3	280/254
21a/b	9.1/8.6	263/263
22	9.2	220
23	12.1	220
24	14.2	220
25	14.8	220
26	10.9	254
27	8.5	263
28	n.d.	n.d.
29	n.d.	n.d.
30	12.7	254
31	3.6	263
32	3.7	280
33	10.0	310
34	12.5	220
35	14.9	310
36	11.2	220
37	12.2	220
38	n.d.	n.d.
39	n.d.	n.d.

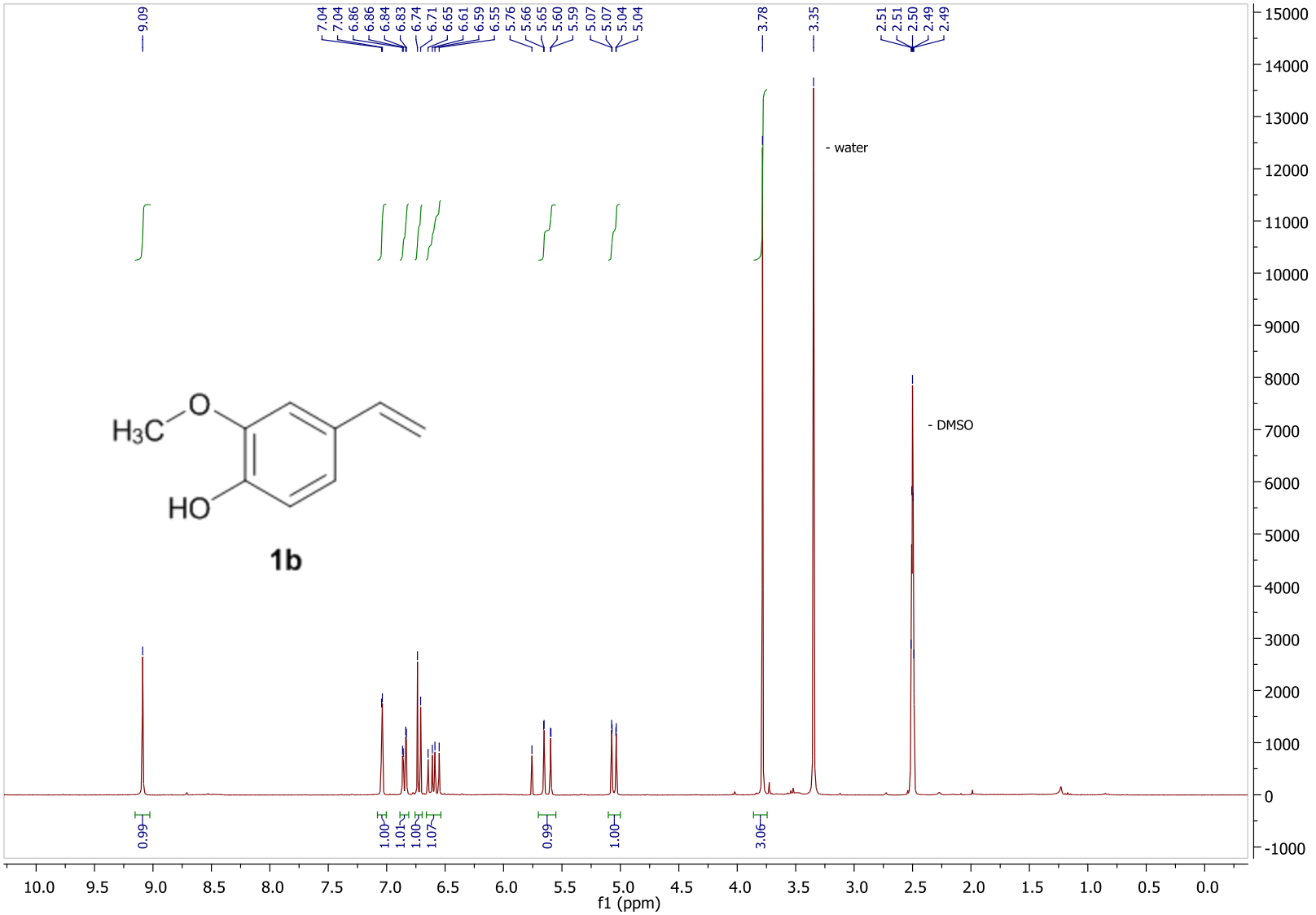

Figure S2. ^{1}H NMR spectrum of **1b** (300 MHz, DMSO-d_6).

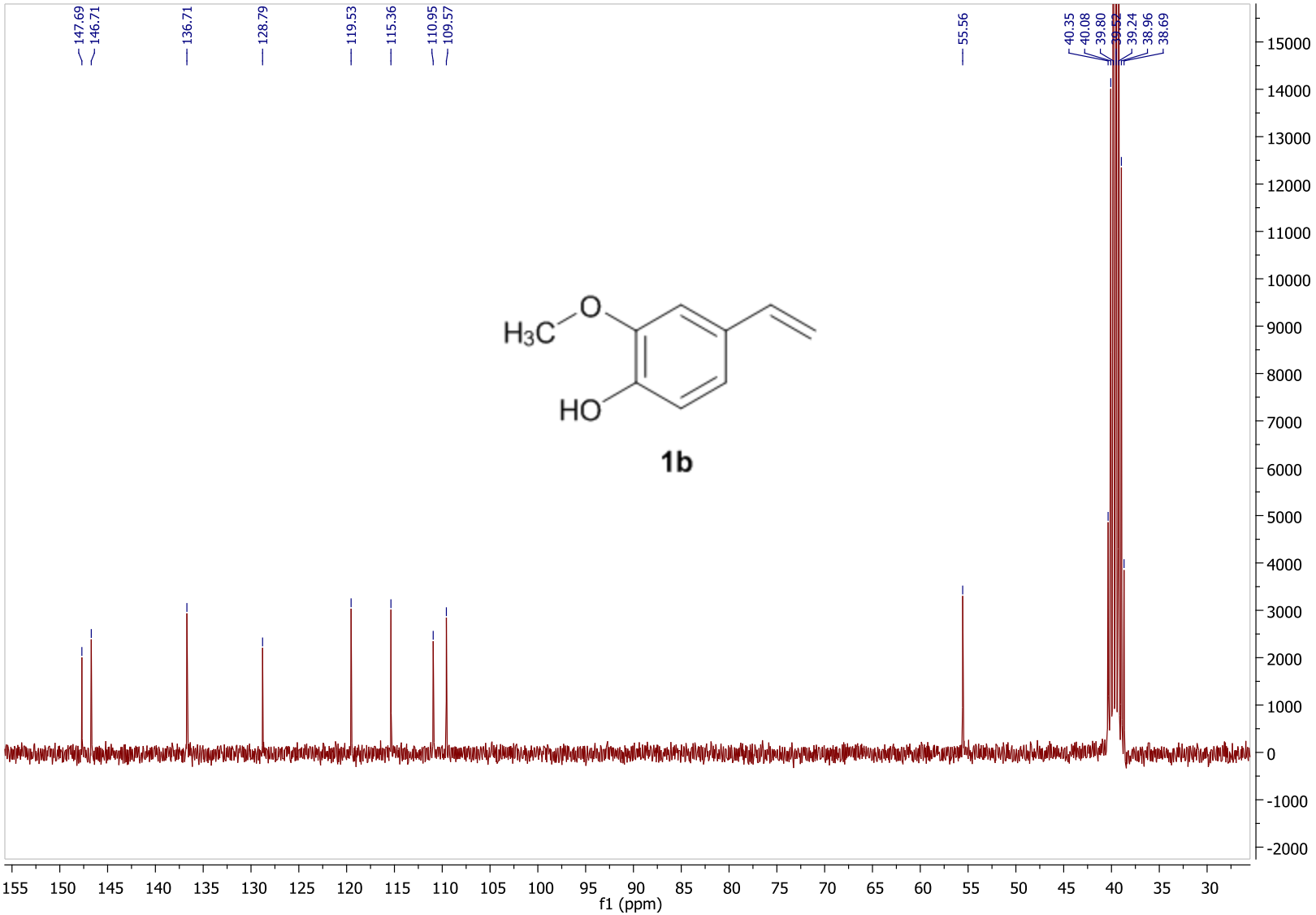

Figure S3. ^{13}C NMR spectrum of **1b** (75 MHz, DMSO-d_6).

References

[1] a) M. Stratford, A. Plumridge, D. B. Archer, *Appl. Environ. Microbiol.* **2007**, *73*, 6534 – 6542; b) S. Coghe, K. Benoot, F. Delvaux, B. Vanderhaegen, F. R. Delvaux, *J. Agric. Food Chem.* **2004**, *52*, 602 – 608; c) N. Mukai, K. Masaki, T. Fujii, M. Kawamukai, H. Iefuji, *J. Biosci. Bioeng.* **2010**, *109*, 564 – 569; d) A. R. Goodey, R. S. Tubb, *J. Gen. Microbiol.* **1982**, *128*, 2615 – 2620; e) P. Richard, K. Viljanen, M. Penttilä, *AMB Express* **2015**, *5*:12.

[2] a) N. Rahimi, R. Karimzadeh, *Appl. Catal. A* **2011**, *398*, 1 – 17; b) S. M. Sadrameli, *Fuel* **2016**, *173*, 285 – 297.

[3] P. Anastas, N. Eghbali, *Chem. Soc. Rev.* **2010**, *39*, 301 – 312.

[4] a) A. Schmid, J. S. Dordic, B. Hauer, A. Kiene, M. Wubbolts, B. Witholt, *Nature* **2001**, *409*, 258 – 268; b) S. M. Thomas, R. DiCosimo, V. Nagarajan, *Trends Biotechnol.* **2002**, *20*, 238 – 242, c) J. M. Woodley, *Trends Biotechnol.* **2008**, *26*, 321 – 327.

[5] K. A. P. Payne, M. D. White, K. Fisher, B. Khara, S. S. Bailey, D. Parker, N. J. W. Rattray, D. K. Trivedi, R. Goodacre, R. Beveridge, P. Barran, S. E. J. Rigby, N. S. Scrutton, S. Hay, D. Leys, *Nature* **2015**, *522*, 497 – 501.

[6] a) D. Leys, N. S. Scrutton, *Curr. Opin. Struct. Biol.* **2016**, *41*, 19 – 26; b) V. Piano, B. A. Palfey, A. Mattevi, *Trends Biochem. Sci.* **2017**, *42*, 457 – 469; c) C. T. Walsh, T. A. Wencewicz, *Nat. Prod. Rep.* **2013**, *30*, 175 – 200; d) M. Baunach, C. Hertweck, *Angew. Chem. Int. Ed.* **2015**, *54*, 12550 – 12552.

[7] a) T. Li, L. Huo, C. Pulley, A. Liu, *Bioorg. Chem.* **2012**, *43*, 2 – 14; b) F. Jordan, H. Patel, *ACS Catal.* **2013**, *3*, 1601 – 1617; c) D. R. Morris, R. H. Fillingame, *Annu. Rev. Biochem.* **1974**, *43*, 303 – 321.

[8] T. J. Erb, *Appl. Environ. Microbiol.* **2011**, *77*, 8466 – 8477.

[9] R. J. Ellis, *Trends Biochem. Sci.* **1979**, *4*, 241 – 244.

[10] a) R. Wohlgemuth, *Curr. Opin. Biotechnol.* **2010**, *21*, 713 – 724; b) J.-M. Choi, S.-S. Han, H.-S. Kim, *Biotechnol. Adv.* **2015**, *33*, 1443 – 1454.

[11] R. Kourist, J.-K. Guterl, K. Miyamoto, V. Sieber, *ChemCatChem* **2014**, *6*, 689 – 701.

[12] a) A. S. Lindsey, H. Jeskey, *Chem. Rev.* **1957**, *57*, 583 – 620; b) Y. Kosugi, Y. Imaoka, F. Gotoh, M. A. Rahim, Y. Matsui, K. Sakanishi, *Org. Biomol. Chem.* **2003**, *1*, 817 – 821.

[13] S. M. Glueck, S. Gümüs, W. M. F. Fabian, K. Faber, *Chem. Soc. Rev.* **2010**, *39*, 313 – 328.

[14] a) K. Plasch, V. Resch, J. Hitce, J. Popłonski, K. Faber, S. M. Glueck, *Adv. Synth. Catal.* **2017**, *359*, 959 – 965; b) J. Ren, P. Yao, S. Yu, W. Dong, Q. Chen, J. Feng, Q. Wu, D. Zhu, *ACS Catal.* **2016**, *6*, 564 – 567; c) C. Wuensch, N. Schmidt, J. Gross, B. Grischek, S. M. Glueck, K. Faber, *J. Biotechnol.* **2013**, *168*, 264 – 270; d) C. Wuensch, S. M. Glueck, J. Gross, D. Koszelewski, M. Schober, K. Faber, *Org. Lett.* **2012**, *14*, 1974 – 1977; e) C. Wuensch, T. Pavkov-Keller, G. Steinkellner, J. Gross, M. Fuchs, A. Hromic, A. Lyskowski, K. Fauland, K. Gruber, S. M. Glueck, K. Faber, *Adv. Synth. Catal.* **2015**, *357*, 1909 – 1918; f) S. E. Payer, S. A. Marshall, N. Bärland, X. Sheng, T. Reiter, A. Dordic, G. Steinkellner, C. Wuensch, S. Kaltwasser, K. Fisher, S. E. J. Rigby, P. Macheroux, J. Vonck, K. Gruber, K. Faber, F. Himo, D. Leys, T. Pavkov-Keller, S. M. Glueck, *Angew. Chem. Int. Ed.* **2017**, *56*, 13893 – 13897; g) K. Kirimura, H. Gunji, R. Wakayama, T. Hattori, Y. Ishii, *Biochem. Biophys. Res. Commun.* **2010**, *394*, 279 – 284; h) L. Pesci, S. M. Glueck, P. Gurikov, I. Smirnova, K. Faber, A. Liese, *FEBS Journal* **2015**, *282*, 1334 – 1345.

[15] M. W. Bhuiya, S. G. Lee, J. M. Jez, O. Yua, *Appl. Environ. Microbiol.* **2015**, *81*, 4216 – 4223.

[16] J. D. Baranowski, P. M. Davidson, C. W. Nagel, A. L. Branen, *J. Food. Sci.* **1980**, *45*, 592 – 594.

[17] S. A. Marshall, K. A. P. Payne, D. Leys, *Arch. Biochem. Biophys*. **2017**, *632*, 209 – 221.

[18] R. A. Leppik, I. G. Young, F. Gibson, *Biochim. Biophys. Acta* **1976**, *436*, 800 – 810.

[19] a) M. D. White, K. A. P. Payne, K. Fisher, S. A. Marshall, D. Parker, N. J.W. Rattray, D. K. Trivedi, R. Goodacre, S. E. J. Rigby, N. S. Scrutton, S. Hay, D. Leys, *Nature* **2015**, *522*, 502 – 506; b) F. Lin, K. L. Ferguson, D. R. Boyer, X. N. Lin, E. N. G. Marsh, *ACS Chem. Biol.* **2015**, *10*, 1137 − 1144.

[20] N. Arunrattanamook, E. N. G. Marsh, *Biochemistry*, **2017**, DOI: 10.1021/acs.biochem.7b01131

[21] S. Kumar, V. Kumar, S. P. Singh, 1,3-Dipolar Cycloadditions, in: *Pericyclic Reactions: A Mechanistic and Problem-Solving Approach*, Academic Press, **2015**, *vol. 1*, pp. 1 – 21 and 244 – 251.

[22] P. Pérez, L. R. Domingo, M. J. Aurell, R. Contreras, *Tetrahedron* **2003**, *59*, 3117 – 3125.

[23] a) A. L Cardoso, T. M. V. D. Pinho e Melo, *Eur. J. Org. Chem.* **2012**, *2012*, 6479 – 6501; b) P. Dauban, G. Malik, *Angew. Chem. Int. Ed.* **2009**, *48*, 9026 – 9029.

[24] H. Pellissier, *Tetrahedron* **2007**, *63*, 3235 – 3285.

[25] a) K. L. Ferguson, N. Arunrattanamook, E. N. G. Marsh, *Biochemistry* **2016**, *55*, 2857 – 2863; b) C.-L. Lan, S.-L. Chen, *J. Org. Chem.* **2016**, *81*, 9289 – 9295.

[26] a) F. Méndez, J. Tamariz, P. Geerlings, *J. Phys. Chem. A* **1998**, *102*, 6292 – 6296, b) D. H. Ess, G. O. Jones, K. N. Houk, *Adv. Synth. Catal.* **2006**, *348*, 2337 – 2361; c) K. N. Houk, *Acc. Chem. Res.* **1975**, *8*, 361 – 369; d) P. K. Chattaraj, *J. Phys. Chem. A* **2001**, *105*, 511 – 513.

[27] K. L. Ferguson, J. D. Eschweiler, B. T. Ruotolo, E. N. G. Marsh, *J. Am. Chem. Soc.* **2017**, *139*, 10972 – 10975.

[28] a) T. Ren, M. Patel, K. Blok, *Energy* **2006**, *31*, 425 – 451; b) M. Tuomaala, M. Hurme, A.-M. Leino, *Appl. Therm. Eng.* **2010**, *30*, 45 – 52.

[29] a) N. Mimura, M. Saito, *Catal. Today* **2000**, *55*, 173 – 178; b) X. Li, J. Feng, H. Fan, Q. Wang, W. Li, *Catal. Commun.* **2015**, *59*, 104 – 107.

[30] a) R. McKenna, D. R. Nielsen, *Metab. Eng.* **2011**, *13*, 544 – 554; b) R. McKenna, B. Thompson, S. Pugh, D. R. Nielsen, *Microb. Cell Fact.* **2014**, *13*:123.

[31] D. R. Vardon, N. A. Rorrer, D. Salvachúa, A. E. Settle, C. W. Johnson, M. J. Menart, N. S. Cleveland, P. N. Ciesielski, K. X. Steirer, J. R. Dorgan, G. T. Beckham, *Green Chem.* **2016**, *18*, 3397 – 3413.

[32] K. A. Curran, J. M. Leavitt, A. S. Karim, H. S. Alper, *Metab. Eng.* **2013**, *15*, 55 – 66.

[33] R. Bernini, E. Mincione, M. Barontini, G. Provenzano, L. Setti, *Tetrahedron* **2007**, *63*, 9663 – 9667.

[34] a) E. Zago, E. Dubreucq, J. Lecomte, P. Villeneuve, F. Fine, H. Fulcrand, C. Aouf, *New J. Chem.* **2016**, *40*, 7701 – 7710; b) P. Terpinc, T. Polak, N. Šegatin, A. Hanzlowsky, N. P. Ulrih, H. Abramovic, *Food Chem.* **2011**, *128*, 62 – 69.